Energy 90 (2015) 1887–1900

Contents lists available at ScienceDirect

Energy

journal homepage: www.elsevier.com/locate/energy

Flexible security-constrained scheduling of wind power enabling time of use pricing scheme

E. Heydarian-Forushani [a], M.E.H. Golshan [a, *], M. Shafie-khah [b]

[a] Isfahan University of Technology, 84156-83111, Isfahan, Iran
[b] University of Beira Interior, R. Fonte do Lameiro, 6201-001, Covilhã, Portugal

ARTICLE INFO

Article history:
Received 22 February 2015
Received in revised form
22 June 2015
Accepted 3 July 2015
Available online 26 July 2015

Keywords:
Power system flexibility
Time of use rates
Security constrained unit commitment
Wind integration

ABSTRACT

Power systems have been conventionally involved with uncertainty and variability due to unpredictable network component contingencies. Recently, large penetration of variable generations has made this variability even worse than before and drives a need for greater flexibility. This paper proposes a flexible security-constrained framework which coordinates supply-side and demand-side in an appropriate way to meet the need for this greater flexibility toward a secure, economic, and green power grid. In the proposed model, conventional units are contributed to flexibility enhancement through providing up and down operational reserves while demand-side flexibility is enabled via an optimal TOU (time of use) pricing scheme as a most prevalent time-based rate demand response programs. Since increasing the share of renewable resources reduces the electricity market prices, it may lead through a situation in which customers do not have enough tendencies to response in expose to the TOU rates. Hence, the paper concludes with determination of optimal TOU tariff rates in the face of high penetration of wind power as well as network contingencies.

1. Introduction

The uncertainty and variability as a consequence of recent deployment of wind power in electricity supply sector besides unexpected network component contingencies may impose essential challenges on TSO(transmission system operator's) performance. High intermittent nature of wind power may disturb power system balance and even enforce TSO to schedule a number of conventional units at non-optimum generation level according to the physical limitation of units such as ramp up/down rates, minimum up/down times, and start-up constraints. In contingency events, TSO also requires a proper response to maintain continuous services and prevent system security endangerment.

In such a situation, increasing operational flexibility is a key solution for mitigating wind power variability and enabling secure operation of power systems. Flexibility should be evaluated from technical, economic, and environmental points of view. Technically, flexibility is required to maintain continuous services in the face of rapid and large fluctuations in both supply and demand sides. Economically, additional cost to provide additional required flexibility should be kept within a plausible range. Moreover, from environmental perspective, lack of flexibility can lead to significant waste of wind generation in the form of wind power curtailment by system operators. However, by obtaining more flexibility from existing conventional units has significant wear-and-tear impacts on existing thermal units and can potentially decrease their expected lifetimes [1]. Reviewing international DR (demand response) experiences reveals that DR programs can be recognized as the potential measures for motion toward a more flexible power grid [2–5]. On this basis, enabling customers' potential via an appropriate DR program can create a new window of opportunity to increase power system flexibility in the face of wind power variability as well as contingency events.

Wind power uncertainty has been incorporated to SCUC (security constrained unit commitment) problem in a number of recent publications [6,7]. Liu and Tomsovic [6] proposed a probabilistic model of SCUC to minimize the cost of energy, spinning reserve, and possible loss of loads considering wind power generation and load uncertainty as well as generator outages. Pozo and Contreras [7] developed a stochastic chance-constrained unit commitment model which includes a novel N-k criterion alongside wind and

* Corresponding author. Department of Electrical and Computer Engineering, Isfahan University of Technology, Isfahan, Iran. Tel.: +98 311 391 5386; fax: +98 311 391 2451.
E-mail address: hgolshan@cc.iut.ac.ir (M.E.H. Golshan).

http://dx.doi.org/10.1016/j.energy.2015.07.014
0360-5442/

load level volatilities. However, the network and line outages have not been considered due to the complexity involved.

Another set of papers have gone a step further by considering higher flexible technologies in their proposed model. PEVs (plug-in electric vehicles) [8], CAES (compressed air energy storages) [9], and hydro units [10] were considered as alternative solutions to solve hourly SCUC, which takes into account the volatility of wind power generation. DR was also integrated to SCUC problem in Refs. [11–13]. Parvania and Fotuhi-Firuzabad [11] presented a stochastic SCUC model in which DR has been modeled by DR providers which aggregate end-use customer responses and participate in the wholesale market on behalf of customers. Operating features of aggregated responsive loads such as bids, hourly profile, and inter temporal properties have been included to SCUC problem in Ref. [12]. Nikzad et al. [13] developed a stochastic method in which the optimum TOU (time of use) rates are determined in SCUC based on grid reliability index. Although the last mentioned publications present comprehensive models, wind power intermittency and environmental considerations have not been addressed in the last three former works.

Wind and load forecast errors have been considered besides component outages in an N-1 contingency model considering an aggregated DR of end-users as a tool for mitigating network constraint violations in Ref. [14]. The fact that has not been referred in the literature is that increasing the integration of wind power to the electricity market, decreases the market clearing price as a consequence of generation cost reduction [15]. This decrease in energy price may alleviate the customer's tendency for participation in DR programs. Therefore, designing an appropriate DR program not only enable the whole demand-side potential but also ensure secure, economic, and less emission pollutant operation of power systems with a considerable share of wind power. On this basis, the current paper presents a flexible stochastic security-constrained scheduling framework to optimize supply-side and demand-side operations simultaneously through an optimal TOU pricing scheme. In short, the main contributions of this paper are highlighted as follows:

1) Determination of optimum TOU tariff rates with application to enable the potential of demand side flexibility in the face of wind power uncertainty as well as large variations in supply (a generation unit or a transmission line outage).
2) Providing additional required flexibility by coordinating generation units and responsive loads to have a secure, economic, and clean power sector.
3) Investigating the effectiveness of two major DR strategies, namely, load curtailment and load shifting on the integration of wind power and contingency condition.

The rest of this paper is organized as follows. Section 2 deals with the proposed framework description and mathematical formulation of the model. Simulation results are presented in section 3 and finally the concluding remarks are given in section 4.

2. Model description and mathematical formulation

The proposed flexible stochastic security-constrained scheduling framework optimizes supply-side and demand-side operations, simultaneously. In order to achieve an optimal supply-side scheduling, a two-stage stochastic programming problem is formulated where the first-stage actually represents the decisions to be declared as the outcome of the day-ahead market several hours before the beginning of the system day it refers to. The second-stage includes possible instances of the wind-power generation as well as network component contingencies that should be all together considered in order to obtain a single day-ahead market clearing. It is worthy to note that the first-stage pertaining to electricity market clearing considers relevant constraints while the second-stage contains the physical network limitations. The demand-side scheduling is also incorporated to the proposed framework using economic model of responsive loads. In this regard, the initial demand profile, the consumer elasticity and the potential of consumers in response to designed TOU mechanism are entered as required inputs. Afterward, optimum TOU tariff-rates of each load bus are determined and the modified demand profile is entered as an input to supply-side scheduling part. The mentioned feedback procedure could link supply-side and demand-side scheduling to ensure an efficient power system operation. Finally, the output variables pertaining to economic, environmental and security operation targets of TSO is extracted as a result. Fig. 1 depicts a schematic representation of the calculation steps.

2.1. TOU demand response program modeling

To model TOU program, the current paper uses the concept of elasticity of demand. Elasticity is defined as the customer's sensitivity to change in electricity tariffs. As the elasticity increases, the load sensitivity to price increases as well. In fact, the elasticity is used to estimate the load reduction and load recovery by DR participants. In this context, the comprehensive economic model of DR programs developed by Aalami et al. [16] is modified to include in the proposed scheduling framework with application to provide a flexible load profile.

The price elasticity of demand in t-th period versus t'-th period which can be defined as it can be seen in Eq. (1). Actually, demand can react to change in electricity tariffs in one of the followings. A set of loads is reduced without recovering it later, the so-called fixed loads. Such loads have sensitivity just in a single period and it is called “self-elasticity”. This value is always negative. Some loads could be moved from the peak periods to off-peak periods as required, namely shiftable loads. Such behavior is called multi period sensitivity and it is evaluated by “cross-elasticity”. This value is always positive. The concepts of self and cross-elasticity are represented by Eq. (2).

$$E(t,t') = \frac{\Delta d(t)}{\Delta \rho(t')} \cdot \frac{\rho_0(t')}{d_0(t)} \quad t' = 1,2,3,\ldots,24 \tag{1}$$

where

$$\begin{cases} E(t,t') \le 0 & if \quad t = t' \\ E(t,t') \ge 0 & if \quad t \ne t' \end{cases} \quad and \quad \frac{\Delta d(t)}{\Delta \rho(t')} = constant \; for \; t,\; t' = 1,2,\ldots,24 \tag{2}$$

If the value of electricity from customer's point of view for using $d(t)$ during hour t is considered as $B(d(t))$, the customer net benefit can be calculated as follows:

$$NB = B(d(t)) - d(t)\cdot\rho(t) \tag{3}$$

In Eq. (3), the first term is dedicated to the net benefit of customer from the use of $d(t)$ in hour t and the last term is related to electricity consumption cost in hour t. It is notable that calculation of $B(d(t))$ is behind the scope of this paper and more details are given in Ref. [17]. In order to maximize the customer's net benefit, the derivate of Eq. (3) should be equal to zero:

$$\frac{\partial NB}{\partial d(t)} = \frac{\partial B(d(t))}{\partial d(t)} - \rho(t) = 0 \tag{4}$$

As a result:

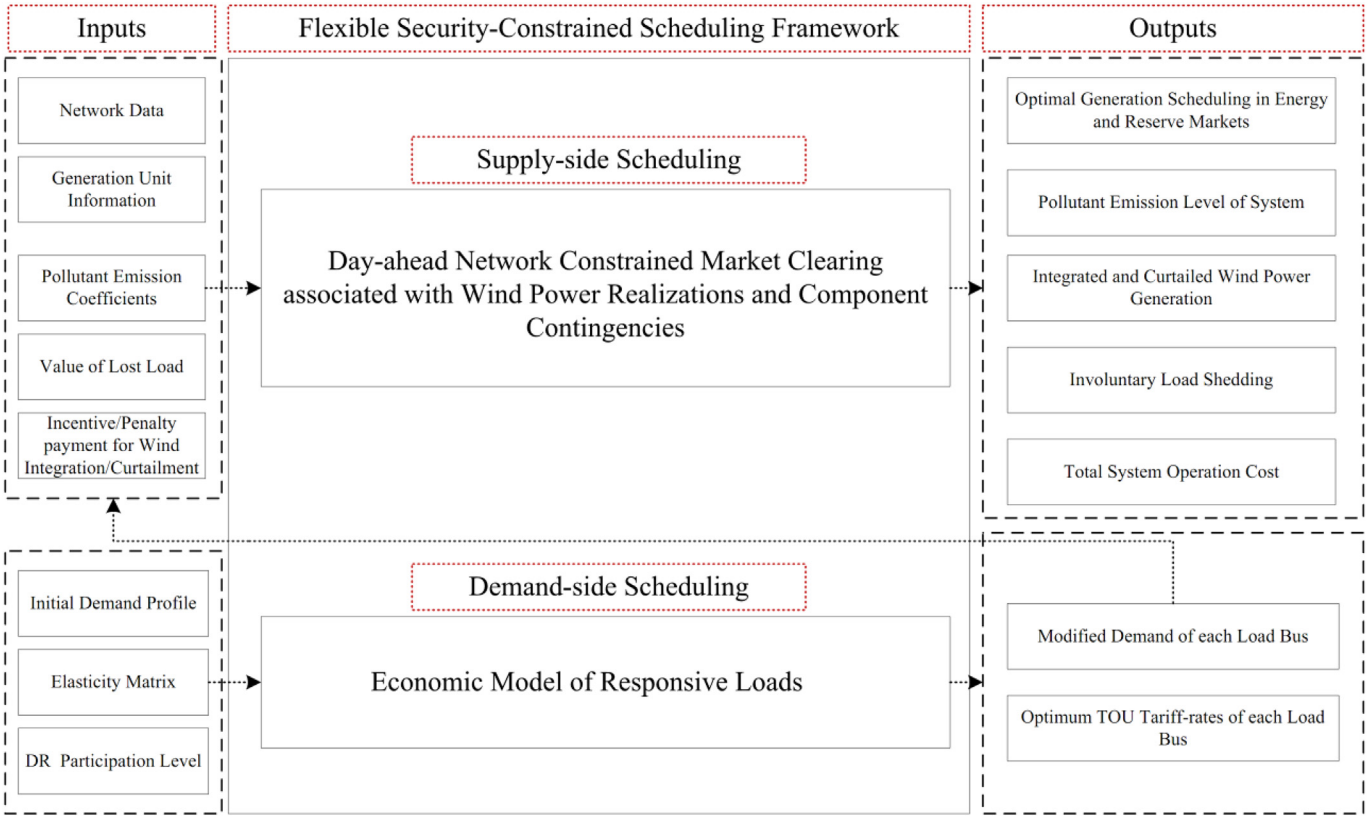

Fig. 1. Schematic representation of the calculation process.

$$\frac{\partial B(d(t))}{\partial d(t)} = \rho(t) \tag{5}$$

Generally, the customer's net benefit is considered as a quadratic function of his/her consumption as follow [17]:

$$B(d(t)) = B_0(t) + \rho_0(t)[d(t) - d_0(t)]\left\{1 + \frac{d(t) - d_0(t)}{2E(t,t)d_0(t)}\right\} \tag{6}$$

By differentiating Eq. (6) and substituting the results in Eq. (5), the initial price-based economic load model will be obtained as shown in Eq. (7):

$$d(t) = d_0(t)\left\{1 + \frac{E(t,t)[\rho(t) - \rho_0(t)]}{\rho_0(t)}\right\} \tag{7}$$

With regard to the concept of the cross elasticity, a change in the electricity price in hour t' may cause the load variation in hour t as represent in Eq. (8).

$$d(t) = d_0(t) + \sum_{\substack{t'=1 \\ t' \neq t}}^{NT} E(t,t')\frac{d_0(t)}{\rho_0(t')}[\rho(t') - \rho_0(t')] \tag{8}$$

As a result of combination of Eqs. (7) and (8), the comprehensive price-based DR model will be obtained as shown in Eq. (9).

$$d(t) = d_0(t)\left\{1 + \sum_{t'=1}^{NT} E(t,t')\cdot\frac{[\rho(t') - \rho_0(t')]}{\rho_0(t')}\right\} \tag{9}$$

By dividing the hourly load profile into three time periods including off-peak, low, and peak time periods, the TOU program model will be obtained which is allocated to appropriate buses as shown in Eq. (10) [13].

$$\begin{aligned} d_b(t) = d_b^0(t)\Bigg\{1 &+ \sum_{t' \in OTP} E(t,t')\cdot\frac{\left[\rho_b^{OTP} - \rho_b^0(t')\right]}{\rho_b^0(t')} \\ &+ \sum_{t' \in LTP} E(t,t')\cdot\frac{\left[\rho_b^{LTP} - \rho_b^0(t')\right]}{\rho_b^0(t')} \\ &+ \sum_{t' \in PTP} E(t,t')\cdot\frac{\left[\rho_b^{PTP} - \rho_b^0(t')\right]}{\rho_b^0(t')}\Bigg\} \end{aligned} \tag{10}$$

Equation (10) indicates the optimum amount of customer consumption at bus b in a 24 h period while participating in TOU program. In order to have an appropriate TOU pricing scheme, inequalities (11–13) must be considered to specify the reasonable range of price in three time periods [13].

$$\rho_b^{OTP} \leq \rho_b^0(t) \tag{11}$$

$$\rho_b^{PTP} \geq \rho_b^0(t) \tag{12}$$

$$\rho_b^{OTP} \leq \rho_b^{LTP} \leq \rho_b^{PTP} \tag{13}$$

Maximum response potential of customers is also modeled through Eq. (14). This equation determines the maximum possible amount of load level that can be decreased in peak periods and recovered in other periods at each bus.

$$-DR_b^{\max}\cdot d_b^0(t) \leq \Delta d_b(t) \leq DR_b^{\max}\cdot d_b^0(t) \tag{14}$$

In order to guaranty the comfort level of customers, Eq. (15) lets the total energy consumption in each bus over the scheduling timeframe remain unchanged. However, if the customers have load reduction potential, the equation should be modified based on their load reduction capability.

$$\sum_{t=1}^{NT} \Delta d_b(t) = 0 \tag{15}$$

2.2. Objective function

The objective function is the expected cost that should be minimized while satisfying several equality and inequality constraints from the TSO's point of view.

$$\begin{aligned} Min \quad & \sum_{t=1}^{NT}\sum_{i=1}^{NG}\left\{\begin{array}{l}\left(SUC_{it} + \underline{F}_i \cdot I_{it} + \sum_{m=1}^{NM}\left(P_{it}^{e}(m)\cdot C_{it}^{e}(m)\right)\right) \\ +\left(C_{it}^{U}\cdot SR_{it}^{U} + C_{it}^{D}\cdot SR_{it}^{D}\right) \\ +\left(\underline{Em}_i \cdot I_{it} + \sum_{m=1}^{NM}\left[ECC^{SO_2}\cdot\left(P_{it}^{e}(m)\cdot e_i^{SO_2}(m)\right) + ECC^{NO_x}\cdot\left(P_{it}^{e}(m)\cdot e_i^{NO_x}(m)\right)\right]\right)\end{array}\right\} \\ & + \sum_{s=1}^{NS}\omega_s \cdot \left\{\begin{array}{c} + \sum_{t=1}^{NT}\sum_{i=1}^{NG}\left(sr_{its}^{U}\cdot C_{it}^{UE} + sr_{its}^{D}\cdot C_{it}^{DE}\right) \\ + \sum_{t=1}^{NT}\sum_{f=1}^{NWF}\left(\pi_{FIT}\cdot W_{fst}^{\text{int}} + \pi_{cur}\cdot W_{fst}^{curt}\right) \\ + \sum_{t=1}^{NT}\sum_{b=1}^{NB}\left(VOLL_{bt}\cdot LS_{bts}\right)\end{array}\right\} \end{aligned} \tag{16}$$

The objective function includes two stages. The first stage is pertaining to the electricity market costs and emission generated by units which is not dependent on scenario's realization. In detail this stage is included in the start-up, energy, up- and down-spinning reserves capacity costs, and eventually emission cost which is approximated in a piecewise manner similar to cost function. The second stage that has considered ω_s probability in the objective function is corresponded to scenarios realization. The first line in this part of objective function is associated with deployed up- and down-spinning reserve costs in scenario s. In order to encourage wind generation units to participate more actively in power production, the most well-known incentive mechanism so-called Feed-In-Tariff (FIT) is considered in the second line. Since there may be moments in the scheduling horizon that operation constraints do not allow the integration of wind power to generate, wind power curtailment cost is also considered in the second line. Finally, the last term is associated with involuntary load shedding cost. The objective function should be minimized considering Eqs. 10–15 and the constraints are described as follows:

2.2.1. First-stage constraints

The first stage constraints pertaining to the electricity market and not depending on scenarios occurrence are presented as follows:

- Generation units start-up cost constraints

$$0 \le SUC_{it} \le C_i^{ST}\left(I_{it} - I_{i,t-1}\right) \tag{17}$$

- Market balance constraints

In fact, the system power balance constraint in the first stage is the representation of the market so that the network constraints are not observed in this stage and the mentioned constraints are enforced in the second stage. Indeed, the network constraints for the realization of each scenario of wind power and component outages will be satisfied in the second stage of the proposed model.

$$\sum_{i=1}^{NG} P_{it}^{tot} + \sum_{f=1}^{NWF} P_{ft}^{wind} = \sum_{b=1}^{NB} d_b(t) \tag{18}$$

where $d_b(t)$ is the modified demand of bus b at hour t after implementing optimal TOU program as represent in Eq. (10).

Thermal units' power, P_{it}^{tot}, can be linearly formulated by Eqs. (19) and (20).

$$P_{it}^{tot} = P_i^{\min}\cdot I_{it} + \sum_{m=1}^{NM} P_{it}^{e}(m) \tag{19}$$

$$0 \le P_{it}^{e}(m) \le P_i^{\max}(m) \tag{20}$$

- Wind generation limit

$$0 \le P_{ft}^{wind} \le P_f^{install} \tag{21}$$

In Eq. (21), $P_f^{install}$ is a parameter submitted as a part of wind farm energy offer. In this paper, we consider the value of this parameter equal to the installed capacity of wind farms.

- Spinning and non-spinning reserve constraints

In order to ensure reliable operation of system to cope with wind power uncertainty and the component outages simultaneously, both the up-spinning reserve and down-spinning reserve are considered. Equations (22) and (23) express the up-spinning and down-spinning reserve capacity limits. In addition, the spinning reserve market lead time is assumed to be τ as shown in Eqs. 24 and 25.

$$P_{it}^{tot} + SR_{it}^{U} \le P_i^{\max}\cdot I_{it} \tag{22}$$

$$P_{it}^{tot} - SR_{it}^{D} \geq P_i^{\min} \cdot I_{it} \tag{23}$$

$$0 \leq SR_{it}^{U} \leq RU_i \times \tau \tag{24}$$

$$0 \leq SR_{it}^{D} \leq RD_i \times \tau \tag{25}$$

- Generation unit up and down constraints

$$P_{it}^{tot} - P_{i,t-1}^{tot} \leq RU_i \cdot I_{it} + P_i^{\min} \cdot (1 - I_{i,t-1}) \tag{26}$$

$$P_{i,t-1}^{tot} - P_{it}^{tot} \leq RD_i \cdot I_{i,t-1} + P_i^{\min} \cdot 1 - I_{it}\Big) \tag{27}$$

- Generation unit minimum up and down time constraints

$$\sum_{t'=t+2}^{t+MUT_i} (1 - I_{it'}) + MUT_i \cdot (I_{it} - I_{i,t-1}) \leq MUT_i \tag{28}$$

$$\sum_{t'=t+2}^{t+MDT_i} I_{it'} + MDT_i \cdot (I_{i,t-1} - I_{it}) \leq MDT_i \tag{29}$$

2.2.2. Second-stage constraints

Constraints involving scenarios realization are given below as the second stage constraints.

- DC power flow equation in scenarios

The hourly generation and load dispatch in each scenario must satisfy power balance constraint at each bus. In this regard, DC load flow equation is applied as it can be seen in Eq. (30).

$$\sum_{i \in G_b} \xi_i^G P_{it}^{tot} + \sum_{i \in G_b} sr_{its}^{U} - \sum_{i \in G_b} sr_{its}^{D} - d_b(t) + LS_{bts} + \left[W_{st}^{\text{int}} - W_{st}^{curt}\right]\Big|_{b=wind-bus} = \sum_{l \in L_b} F_{lts} \tag{30}$$

$$F_{lts} = \xi_l^L [(\delta_{bts} - \delta_{b'ts})/X_l] \tag{31}$$

Here, in order to consider outage of generation units and transmission lines, two binary parameters called ξ_i^G and ξ_l^L are considered, respectively. ξ is set to 0 if component outage has occurred and it is assumed as 1 otherwise.

- Transmission line flow limit

$$-F_l^{\max} \leq F_{lts} \leq F_l^{\max} \tag{32}$$

- Deployed up- and down-spinning reserve limit

$$0 \leq sr_{its}^{U} \leq \xi_i^G SR_{it}^{U} \tag{33}$$

$$0 \leq sr_{its}^{D} \leq \xi_i^G SR_{it}^{D} \tag{34}$$

- Involuntary load shedding limit

The amount of load shedding in each scenario at each bus should be less than the amount of modified load of the bus after implementation of TOU as it can be seen in Eq. (35).

$$0 \leq LS_{bts} \leq d_b(t) \tag{35}$$

- Wind power constraints

The amount of integrated wind power of each wind farm must be less than the available wind generation. Also, just both the amounts of curtailed wind power and integrated wind power of each wind farm are positive variables. These issues are addressed in Eq. (36). Eq. (37) ensures that the summation of integrated and curtailed wind power of wind farms will be less than the available wind power.

$$0 \leq W_{fst}^{\text{int}} \leq W_{fst}^{\max}, \quad W_{fst}^{curt} \geq 0 \tag{36}$$

$$W_{fst}^{\text{int}} + W_{fst}^{curt} \leq W_{fst}^{\max} \tag{37}$$

Based on the flexibility concept definition that was presented in this paper, operational flexibility should be ensured optimal operation of power system from technical, economic, and environmental point of view. On this basis, in order to consider the priorities set by TSOs, this paper utilizes some additional constraints.

- Security index

The expected load not supplied (ELNS) index is applied in order to measure system security which has been introduced by Bouffard and Galiana firstly [18] as represent in Eq. (38).

$$ELNS_t = \sum_{b=1}^{NB} \sum_{s=1}^{NS} \omega_s \cdot LS_{bts} \tag{38}$$

- Total emission

In this paper, NO_x and SO_2 emissions are considered as two most popular pollutants to conduct emission. Total system emission in a 24-h scheduled horizon is calculated by Eq. (39).

$$Emission = \sum_{t=1}^{NT} \sum_{i=1}^{NG} \left[\sum_{m=1}^{NM} \left[\left(P_{it}^{e}(m) \cdot e_i^{SO_2}(m) \right) + \left(P_{it}^{e}(m) \cdot e_i^{NO_x}(m) \right) \right] \right] \tag{39}$$

3. Numerical studies

The modified single area IEEE Reliability Test System (RTS-79) and modified RTS-96 which is a multi-area reliability test system created as a consequence of linking various single RTS-79 areas are used to illustrate the performance of the proposed method. This test system is selected due to its similarity to a real large-scale power network containing a variety of generation technologies. All the case studies are modeled in General Algebraic Modeling System (GAMS) environment and solved using CPLEX 12.5.0 as an MILP solver.

3.1. Modified IEEE RTS-79

The modified IEEE RTS-79, in which the 6 hydro units have been removed, as illustrated in Fig. 2, is used to demonstrate the features of the proposed model. The modified system includes 26 generation units, 2 wind energy units, 38 branches, and 17 loads. All the required data of the mentioned test systems including generation units and network parameters are taken from Ref. [19]. It is presumed that generation units submit their energy offers by three linear segments between the minimum and maximum generation units capability based on their marginal incremental costs given in Ref. [20]. In addition, it is assumed that all generation units offer capacity of up- and down-spinning reserves at the rates of 40% of their highest incremental cost of producing energy. Furthermore, the deployed up- and down-spinning reserve costs are considered equal to the highest incremental cost of energy production.

The hourly load corresponds to a weekend day in winter as given in Ref. [19] while the peak of the day is assumed 2670 MW. It is noteworthy that the load curve is divided into three periods: low-load period (1:00–8:00), off-peak period (9:00–16:00), and peak period (17:00–24:00). Furthermore, the self and cross price elasticity values are extracted from Ref. [16].

In this paper, two most popular pollutants are considered to conduct emission cost calculation. The pollution coefficients are approximated by a piecewise linearization technique and directly extracted from Ref. [20]. Moreover, the environmental cost coefficient of pollutants are considered to be 0.5 $/kg and 3 $/kg for SO_2 and NO_x emissions, respectively [21]. In order to show the effect of wind power penetration on the system operation, we add two wind farms at Bus 2 and Bus 22. Each wind farm installed capacity is 600 MW. Therefore, the total wind power capacity is 1200 MW, nearly 28% of total generation capacity which is corresponded to the future targets set by many developed countries to achieve large-scale integration of wind power. The FIT incentive value and wind power curtailment cost are assumed to be 17.5 and 30 $/MWh, respectively. The value of wind curtailment cost is chosen

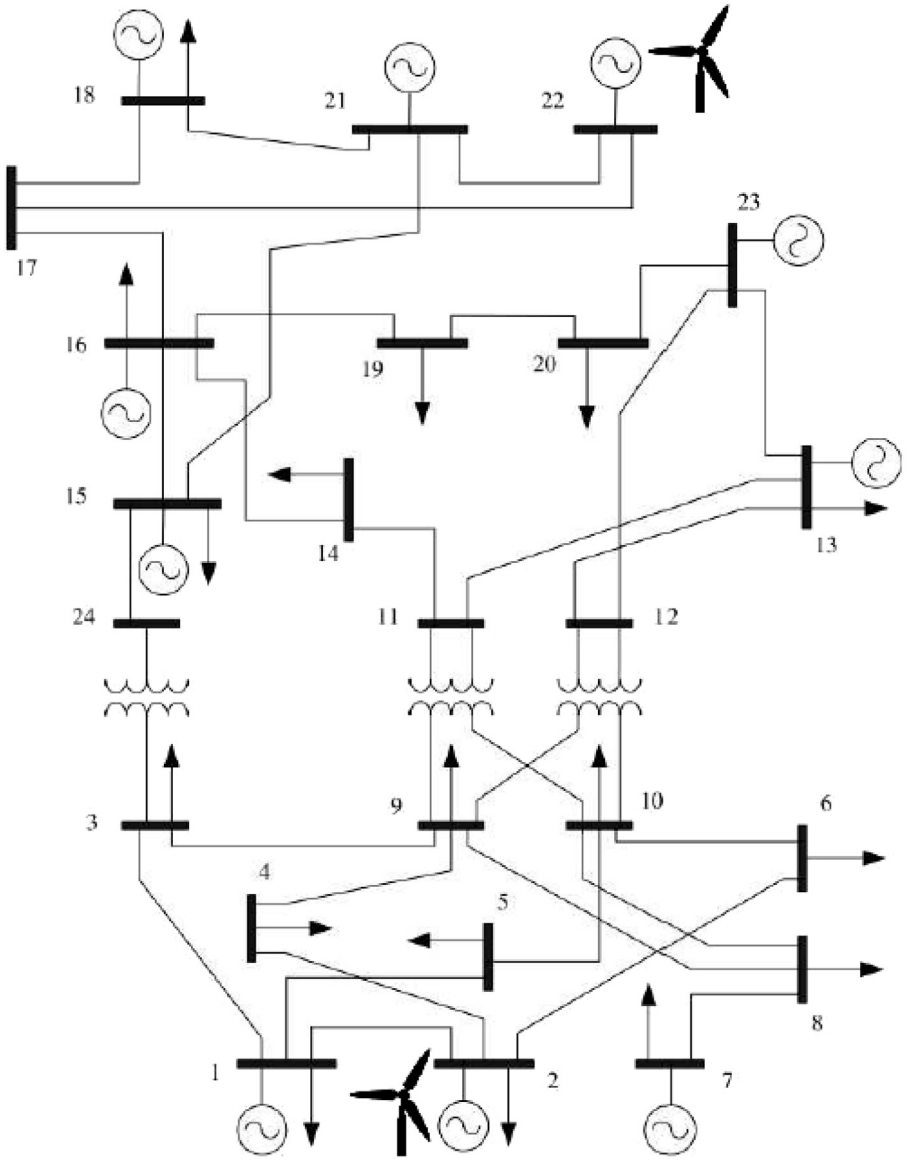

Fig. 2. Modified IEEE RTS-79.

higher than the value of FIT incentive with the aim of persuading the system operator to integrate maximum available wind power into the grid.

To model hourly generation of wind farms, a Weibull distribution has been considered for wind speed as in Ref. [22] and a similar procedure as it has been described in Ref. [22] is utilized to obtain corresponding wind power. Afterward, a scenario generation technique based on Roulette Wheel Mechanism (RWM) is applied here in order to model wind power uncertainty [23]. For the sake of simplicity and reducing computational complexity, the generated scenarios have been decreased to ten independent scenarios using K-means clustering approach [24]. The VOLL is set to 200 $/MWh at each load bus. Also, the initial electricity prices (i.e.$\rho_b^0(t)$) are assumed to be 19 $/MWh equal to the average of hourly electricity prices before optimal TOU implementation without considering component outages occurrence which is the same for all buses due to the lack of network congestion.

In order to evaluate the effectiveness of the proposed model on providing operational flexibility from technical, economic, and environmental perspectives, the following four case studies are considered as indicated in Table 1.

Case 1 and case 3 are referred to flat rate tariffs. It should be mentioned that fixed rate tariffs are the simplest form of supplying electrical energy in which consumers can consume any amount of electrical energy at an agreed fix rate. In these cases, the average of hourly electricity prices over 24 h scheduling horizon is considered as flat rate. In case 1, the wind power uncertainty is considered through scenario generation technique while case 3 contains three N-1 contingencies include the outage of generators at Buses 1, 15 and the outage of transmission line between Buses 14–16 along with wind power scenarios. It should be noted that there is not any limitation in selection of the mentioned contingencies and any other combination of network contingencies can be taken into account without losing comprehensiveness. Moreover, it is worthy to note that although the current paper uses stochastic programming approach, for the sake of simplicity and diminish computation complexity, the component outages are considered in their deterministic form using N-1 criterion.

Case 2 and case 4 are the same as the former cases except that in these two cases demand side flexibility is also incorporated through optimal TOU pricing scheme. To this end, the tariffs of electricity consumption are optimally arranged in a way that the lowest operation cost is achieved. The maximum DR potential is assumed 10% for all load buses. In other words, only 10% of consumers are modeled as responsive demands.

Case 1: This case evaluates the impact of wind power variations on system operation under a flat rate price scheme. In other words, demand-side flexibility is not incorporated into the system operation in this case, hence, the additional required flexibility as a consequence of wind power volatility is provided by conventional supply-side power plants completely through operational reserve. The calculated total operation cost is $ 737810 with an expected involuntary load shedding of 1.6 MWh due to infeasibilities in wind power generation. Moreover, the wind power curtailment is 7.49 MWh and the value of emission is 124.03 tons. The hourly demand, operation cost, and emission in case 1 are illustrated in Fig. 3. As it can be seen, in case 1, the profile of operation cost and emission is significantly similar to the load cure.

Table 1
Statement of case studies.

Case no.	Pricing scheme	Wind uncertainty	N-1 contingency
1	Flat rate	Yes	No
2	Optimal TOU	Yes	No
3	Flat rate	Yes	Yes
4	Optimal TOU	Yes	Yes

Case 2: In this case, 10% of the hourly load at all buses is considered as responsive demand which may be shifted from peak hours to off-peak hours without any change in energy consumption level. In this study system, operator can provide additional required flexibility by coordinating supply-side and demand-side flexibility options. Accordingly, the operation cost is dropped to $ 734,610. Moreover, the expected involuntary load shedding and the wind power curtailment values are equal to 1.43 MWh and 5.38 MWh, respectively. Enabling potential of demand-side flexibility not only ensures secure and economic operation of power grid, but also brings environmental benefits by decreasing 3.63 tons pollutant emission per day. It is noteworthy that, hourly load standard deviation is reduced from 302.61 MW to 227.48 MW as a result of applying an appropriate TOU pricing scheme which confirms the potential of demand-side flexibility in providing a flatter load profile in systems with high penetration of wind power. The calculated TOU rates for case 2 are reported in Table 2. Another set of loads may be reduced without recovering it later so-called curtailable loads. Assume that 5% of load level is curtailable loads and the rest are shiftable loads. As a result, the total operation cost is $ 673,670 (i.e., 8.7% decreases in operation cost) with pollutant emission of 88.1 tons which is less than when the load just was shifted.

The demand response to these rates has been determined for each load bus according to TOU model given in Eq. (10), afterward the total system modified load curve is obtained as it is illustrated in Fig. 3a. As it can be seen, the demand during peak period is reduced and recovered later in low-load hours. This is due to the fact that, the obtained TOU rates in peak period are higher than the flat rate except in some buses and it causes the demand to be decreased in this period and recover in low-load period where the obtained TOU rates are generally lower than the flat rate. Therefore, in general, the load in peak period decreases and the load in low-load period increases in comparison with case 1. It is noteworthy that, the calculated TOU rates are different for various load buses to achieve an optimal solution. In order to evaluate the effectiveness of provided flexibility because of TOU implementation on operation cost and pollutant emission, the hourly total operation cost and pollutant emission is compared in the two mentioned cases as shown in Fig. 3b and c, separately.

As it can be seen in Fig. 3, coordinated scheduling of supply-side and demand-side can lead to operation cost reduction as well as pollutant emission restriction in peak hours by shifting load to the low-load hours. It is notable that the obtained benefits are higher if consumers have the potential of load curtailment alongside load shifting. According to Fig. 3b, implementation of TOU pricing scheme by using shiftable load cause the system operation cost to be reduced in peak hours and to become approximately equal to the cost at off-peak hours. In other words, the operation cost is also shifted from peak hours to the off-peak ones. As it can be seen in Fig. 3c, shiftable load causes that the amount of emission in off-peak hours to be increased compared with case 1. However, implementation of curtailabe loads can reduce the emission in both peak and off-peak periods. From another point of view, the obtained results of Table 2 can be investigated vertically instead of horizontally. It means that besides comparing the tariffs in low-load, off-peak and peak-periods; we can compare the calculated tariffs in different buses. The algorithm for reducing the total cost prepares a nice shortcut. It motivates the consumers to decrease their demand in Buses 1–10 (by increasing the tariffs in comparison to flat-rate) and encourages the consumers to increase their demand in Buses 13–20 (by decreasing the tariffs in comparison to

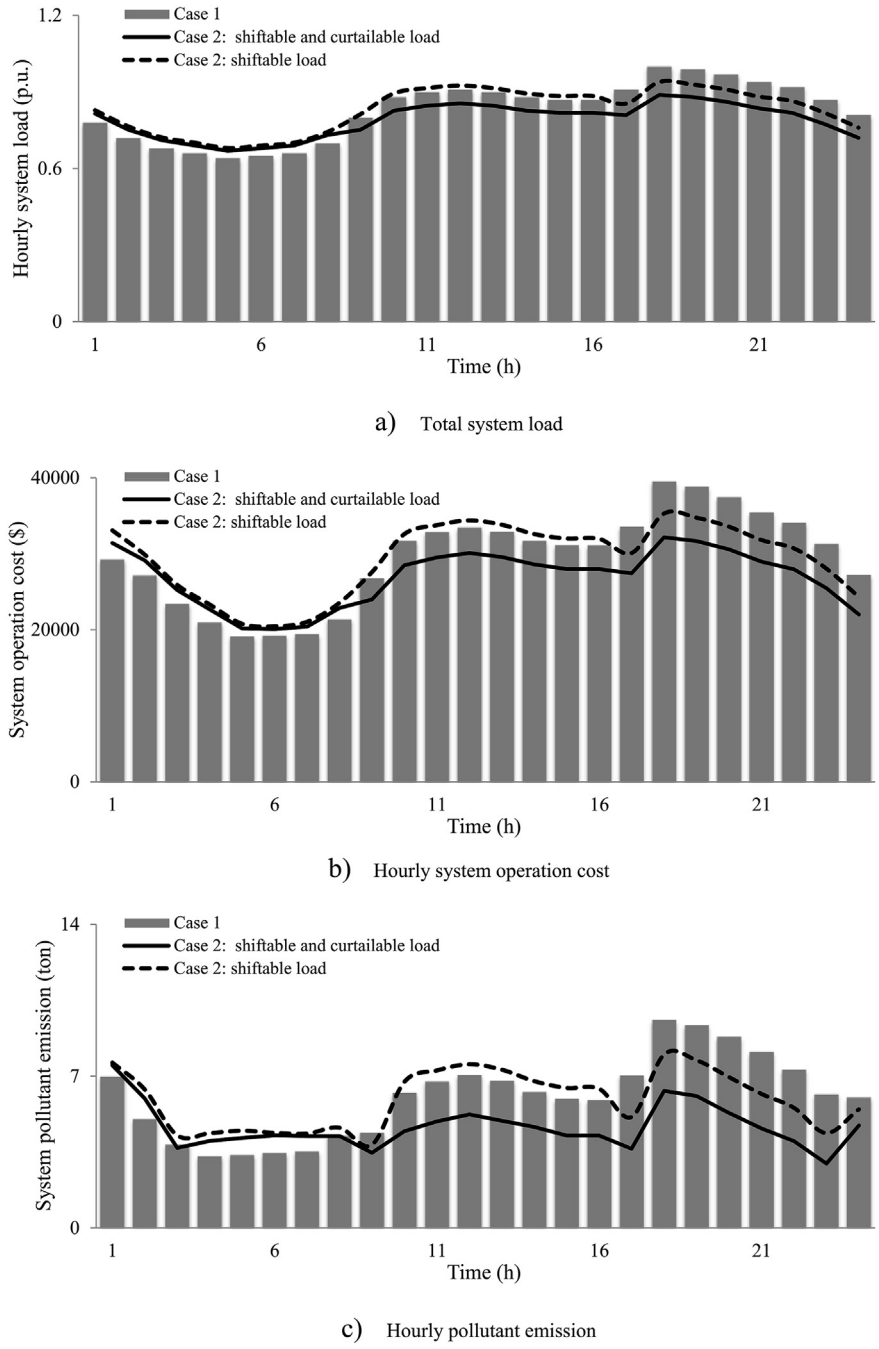

Fig. 3. Comparison of hourly demand, operation cost, and emission in case 1 and case 2 for the RTS-79.

flat-rate). It means a decrease in the power transfer from upside of grid to downside.

The key points here are related to the amounts of installed generation capacity, demand distribution, and generation costs in upside and downside of the grid. For instance, less than 30% of the installed generation capacity belongs to downside of the grid whereas more than 46% of the total demand is related to this part. In addition, the power generation technologies in downside of the grid are more expensive than the upside. In other words, there seem to be two parts in the IEEE RTS-79, one part is load base (downside) and another one generator base (upside). Therefore, in order to find a balance between these two parts, the proposed model motivates the consumers to change their typical consumption pattern using an efficient TOU mechanism. Table 3 compares the loading level of transformers connecting upside of the grid to the downside for each time period. As it can be seen, the transferred power from upside of the grid to downside is decreased in off-peak and peak periods and is increased in low-load period. This may result in diminished generation cost in the expensive side toward a cost-effective power system operation.

To evaluate the cost effectiveness of the proposed model, different terms of operation cost have been presented in Table 4 in details. It is obvious that additional provided flexibility as a consequence of optimal TOU pricing scheme can improve overall system operation condition. The obtained results prove that, load shifting strategy is more effective than the load curtailment

Table 2
Optimal TOU rates ($/MWh) in case 2 for the RTS-79.

Bus no.	ρ_b^{LTP}	ρ_b^{OTP}	ρ_b^{PTP}
1	19	21.7	21.7
2	19	21.7	21.7
3	19	21.7	21.7
4	19	21.7	21.7
5	19	21.7	21.7
6	19	21.7	21.7
7	19	21.7	21.7
8	19	21.7	21.7
9	19	19	21.03
10	19	19.44	21.43
13	16.36	16.36	19
14	17.67	17.67	19
15	16.36	16.36	19
16	16.36	16.36	19
18	16.36	16.36	19
19	16.36	16.36	19
20	16.36	16.36	19

strategy in facilitating wind power integration due to reducing wind power spillage as well as decreasing involuntary load shedding value in the face of wind power uncertainty. Nevertheless, load curtailment has significant effects on the energy and emission reduction and reduces the need for reserve due to the load reduction.

As discussed previously and based on the obtained tariff-rates in Table 2, it can be concluded that consumption reduction in peak hours and consumption enhancement in low-load and off-peak periods are the optimal strategies for TSO to schedule downside and upside of the grid, respectively. On this basis, the impact of proposed coordinated scheduling of supply-side and demand-side on generated power of different buses located in upside and downside of the test system has been indicated in Fig. 4. As it can be observed, reduction of the power generation for downside buses (Buses 1, 2, and 7) in peak period is more impressive than power generation enhancement. On the other hand, the increase in generated power of buses located in upside of the test system (Buses 13, 15, 16, 18, 21, and 23) in low-load and off-peak periods is more remarkable.

Case 3: This case is similar to case 1 with the exception that the effect of network component contingencies are also included into the problem in order to investigate optimal supply-side scheduling in the face of rapid and large fluctuations. Here, we investigate the effect of wind power fluctuations as well as component outages on system operation under a flat rate price scheme. In this condition, TSO must provide additional required flexibility through supply-side unit dispatch to maintain continuous services in a cost effective way. Accordingly, a unit dispatch is obtained with a total operation cost of $1,146,700 which is 55% higher than that of the case 1. Here the cost is higher because the need for maintaining system security in the face of component outages. In other words, the security cost which is imposed to system is equal to $408890. It should be noted that, the amount of involuntary load shedding over the scheduling horizon is 405.96 MWh which can lead to customer dissatisfaction. Moreover, the amount of emission is 216.25 tons which is higher than that of case 1. This is due to the fact that, the TSO has to dispatch more pollutant units in order to maintain continuous services with the least amount of load shedding.

Case 4: In this case, demand-side scheduling is also incorporated into the problem using an efficient TOU pricing scheme. Accordingly, the initial unit commitment is adjusted and loads are shifted as preventive actions. When we consider a 10% load shift, the total operation cost is reduced to $1,057,600. Additional flexibility as a consequence of optimal TOU implementation can significantly improve system security by decreasing the expected load shedding value to 50.65 MWh. Furthermore, the value of emission is diminished to 209.32 tons which is 3.2% less than that of case 3. The optimal TOU rates at each load bus are determined as given in Table 5. It is noteworthy that, if assume that 5% of load have the potential of curtailment and the rest are shiftable loads, the system cost reduces to $972430 with an expected involuntary load shedding of 37.46 MWh.

Table 3
Upside to downside connection transformer loading level in case 1 and case 2 for the RTS-79.

Case no.	Time period	Transformer loading (MVA)					
		B3–B24	B9–B11	B10–B12	B9–B12	B10–B11	Total
Case 1	low load	1001	575	812	635	752	3776
	off-peak	1563	894	1293	984	1203	5937
	peak	1561	885	1303	1001	1188	5938
Case 2: Shiftable	low load	1024	585	842	660	766	3877
	off-peak	1373	783	1174	914	1043	5286
	peak	1481	826	1203	919	1111	5540
Case 2: Shiftable and curtailable	low load	1064	613	868	678	804	4026
	off-peak	1286	705	1017	773	948	4729
	peak	1423	780	1109	830	1059	5201

Table 4
Different terms of operation cost in the face of wind power uncertainty for the RTS-79.

Pricing scheme	Case 1: Flat rate	Case 2: Optimal TOU	
		Shiftable load	Shiftable and curtailable load
Startup cost ($)	156,467	156,467	156,467
Energy cost ($)	302,024	300,152	269,172
Capacity reserve cost ($)	8785	9059	8458
Deployed reserve cost ($)	12,821	13,649	12,391
Emission cost ($)	269,930	267,540	239,430
FIT cost ($)	128,055	128,116	128,090
Load shedding cost ($)	325	286	325
Wind spillage cost ($)	225	161	165

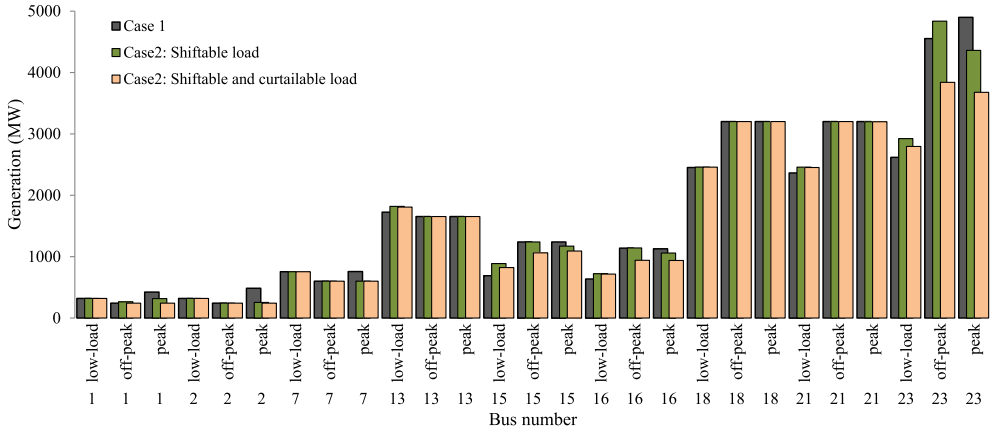

Fig. 4. Power generation of system buses in case 1 and case 2 for the RTS-79.

Table 5
Optimal TOU rates ($/MWh) in case 4 for the RTS-79.

Bus no.	ρ_b^{LTP}	ρ_b^{OTP}	ρ_b^{PTP}
1	16.67	16.67	20.72
2	16.67	16.67	20.72
3	16.52	16.52	19.92
4	17.21	21.13	21.34
5	19	21.7	21.7
6	19	21.7	21.7
7	16.36	16.36	19
8	19	21.7	21.7
9	17.8	21.48	21.48
10	19	21.7	21.7
13	17.24	21.38	21.38
14	19	21.7	21.7
15	16.36	16.36	19
16	16.36	16.36	19
18	16.31	16.36	19
19	16.36	16.36	19
20	16.36	16.36	19

As it can be seen in Table 5, the change in the initial price is higher than that of case 2, when the system just faced with wind power uncertainty. Moreover, it can be seen that the difference between downside and upside of the grid in this case is lower than case 2. It is because of contingencies on Buses 1, 15. These contingencies changed the solution to split the network into two major parts, because it could change the power balance totally. However the prices in upside (Buses 15, 16, 18, 19, and 20) are still similar to case 2. It means the contingencies mostly changed the downside generation. Table 6 indicates the amount of transferred power between upside and downside of the grid in the presence of contingency. As it can be observed the amount of transferred power between upside and downside of the grid decreased drastically in comparison with previous study (non-contingency occurrence). This is due to the fact that, system security has a higher priority compared to economic objectives in contingency events.

In order to explore the effectiveness of the proposed model as a flexible tool in the face of component contingencies as well as stochastic wind power, the hourly system demand profile, operation cost and pollutant emission is compared as given in Fig. 5a–c, respectively. As it can be seen, the load shifting strategy in case 4 causes the demand to be shifted from the peak hours to the low-load period, in contrast to case 2 that shifts the demand from the peak period to off-peak hours. This causes that the operation cost in case 4 with considering shiftable load maintains lower than that in case 3 in off-peak period. Instead, the operation cost is increased in low-load period. According to Fig. 5 c, the profile of pollutant emission is not similar to the load curve and the operation cost pattern. In case 3, the emission is almost equal in all peak and off-peak hours. The reason is that, the amount of generation during peak and off-peak periods is approximately equal, as indicated in Fig. 6. According to Fig. 6, the generation in off-peak and peak periods is similar for buses 2, 7, 13 and 23. It is noteworthy that, the amount of reduction in pollutant emission as a consequence of incorporating demand-side scheduling in these cases is less than that of case 1 and case 2. This is due to the fact that maintaining system security has the highest priority from TSO's point of view during contingencies occurrence. Furthermore, comparison of operation cost in Fig. 5b depicts that load curtailment is a more effective strategy in comparison with load shifting in the face of component contingencies, particularly in peak hours.

The terms of operation cost are compared in case 3 and case 4 as represented in Table 7. As it can be observed in Table 7, the additional flexibility as a result of coordinated scheduling of supply-side

Table 6
Upside to downside connection transformer loading level in case 3 and case 4 for the RTS-79.

Case no.	Time period	Transformer loading (MW)					
		B3–B24	B9–B11	B10–B12	B9–B12	B10–B11	Total
Case 3	low load	37	205	439	418	80	1180
	off-peak	97	403	893	886	378	2657
	peak	232	497	963	929	430	3051
Case 4: Shiftable	low load	114	301	531	587	245	1780
	off-peak	233	434	875	904	405	2851
	peak	141	409	869	887	391	2696
Case 4: Shiftable and curtailable	low load	52	192	412	467	138	1261
	off-peak	206	436	798	875	359	2674
	peak	151	391	818	833	375	2568

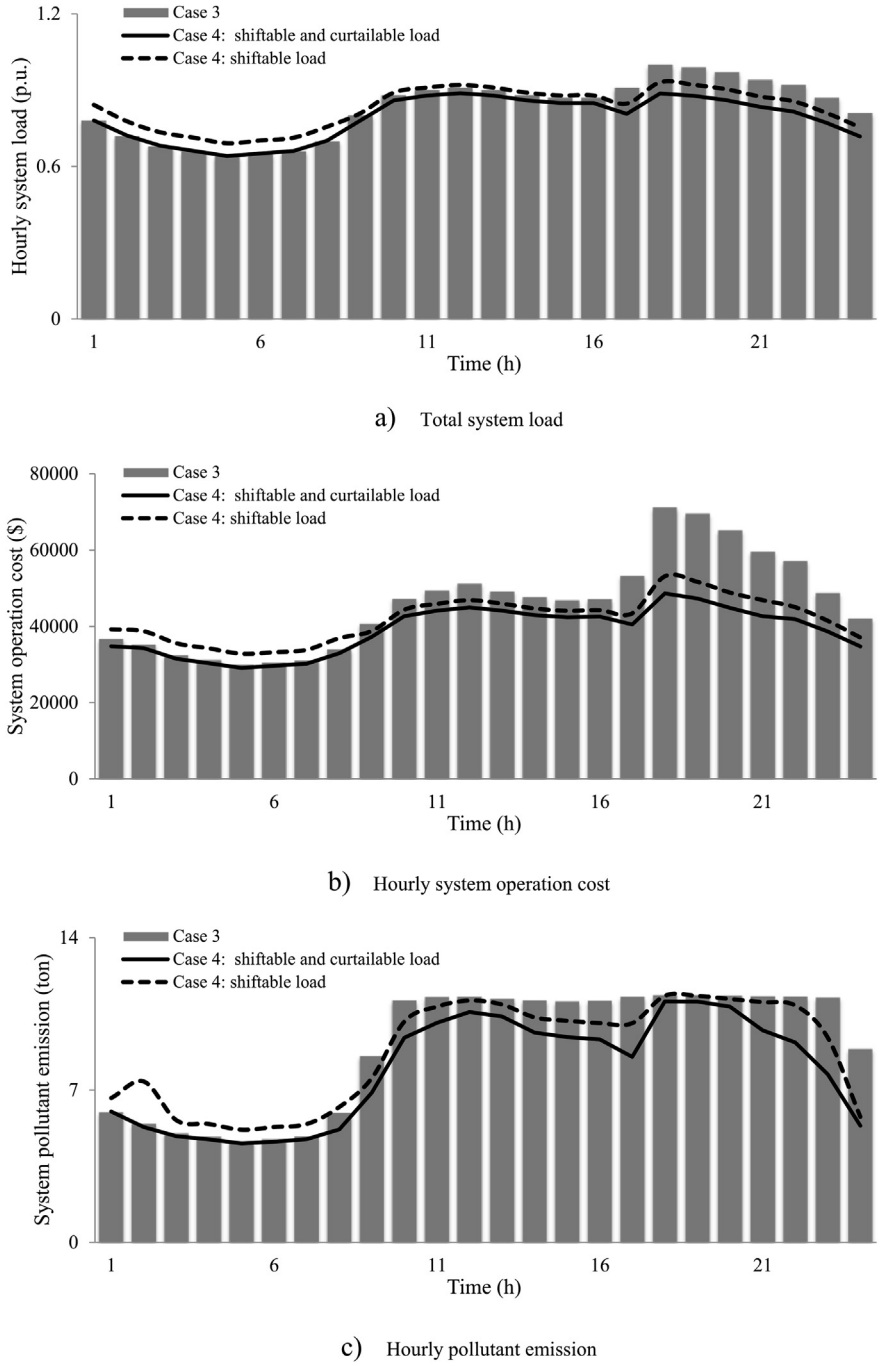

Fig. 5. Comparison of hourly demand, operation cost, and emission in case 3 and case 4 for the RTS-79.

and demand-side can improve power system operation in economic, technical, and environmental aspects.

The difference of startup cost in the presence of contingency events is a key factor in this table. This is due to the fact that TSO has to commit expensive units in contingency events in order to maintain system security. The generation units located in Bus 1 and Bus 2 (I6–I9) are the most expensive units of the grid. In case 3, I7 and I9 are commited in all the 24 h while I6 and I8 are scheduled for hours 10:00 to 23:00. In case 4 when the load can shift between periods, all the mentioned units are commited for only 3 h in a day from 18:00 to 20:00. Hence, the units are committed and decommitted more frequently and consequently the startup cost is increased. In the case of load curtailment, the mentioned units are not committed at all. Therefore the startup cost of the units in this case is less than the other cases. The same discussion also can be exerted for energy cost reduction as a consequence of load shifting and load curtailment strategies as it can be seen in Table 7. Moreover, the system security is significantly improved. For instance, the load shedding cost is decreased more than 60% and 80% because of load shifting and load curtailment, respectively. Therefore it can be concluded that load curtailment strategy is a more effective tool in contingency events.

As it can be seen in Fig. 6, since the generation units located in Bus 1 and Bus 2 (I6–I9) are the most expensive units of the grid, the

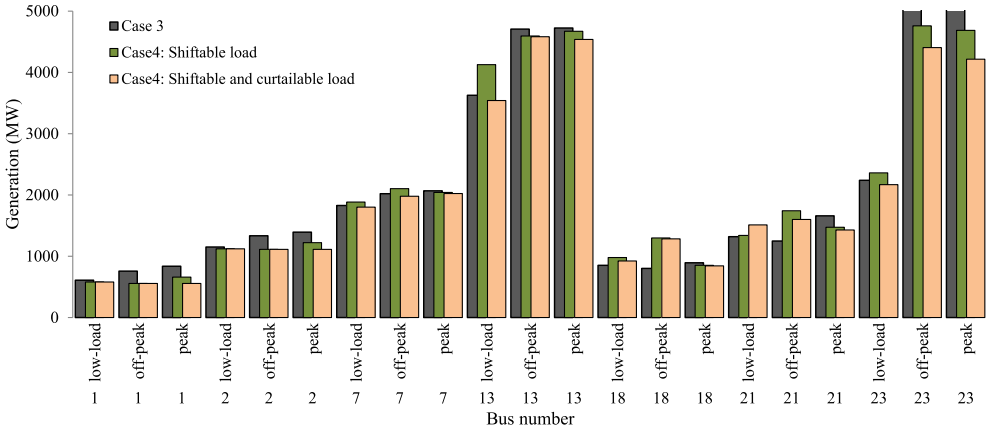

Fig. 6. Power generation of system buses in case 3 and case 4 for the RTS-79.

Table 7
Different terms of operation cost in the face of stochastic wind power and N-1 contingencies for the RTS-79.

Pricing scheme	Case 3: Flat rate	Case 4: Optimal TOU	
		Shiftable load	Shiftable and curtailable load
Startup cost ($)	12,856	13,983	12,914
Energy cost ($)	515,814	497,471	454,212
Capacity reserve cost ($)	10,503	11,262	11,652
Deployed reserve cost ($)	21,766	22,625	22,761
Emission cost ($)	359,020	346,780	321,730
FIT cost ($)	126,540	126,980	127,080
Load shedding cost ($)	97,386	36,422	20,191
Wind spillage cost ($)	2808	2059	1892

generated power of these buses is decreased because of the proposed approach even in off-peak hours. Following these buses, Bus 13 and Bus 7 are considered as expensive generations. The total generated power of these buses is decreased more compared to the other ones. It is notable that the generation of Bus 15 and Bus 16 is decreased to zero. This may be due to the outage of generation unit at Bus 15 as well as contingency in transmission line between Buses 14–16 which are more relevant to these buses.

In order to investigate the effects of the proposed framework on the market clearing price, the changes in expected market clearing price is shown in Fig. 7. On this basis, Fig. 7a is obtained from subtraction the market clearing prices in case 2 from those in case 1. Similarly, Fig. 7 b is extracted from subtraction the prices in case 4 from those in case 3. As it can be seen in Fig. 7 a, shiftable loads increase the market prices in the low-load period and decrease the prices in the peak period. According to Fig. 7b, considering the security constraints magnify the impact of the optimal TOU program, on reducing the market prices in both off-peak and peak periods. In addition, it can be concluded that curtailabe loads have less impact on low-load period compared to shiftable loads. In

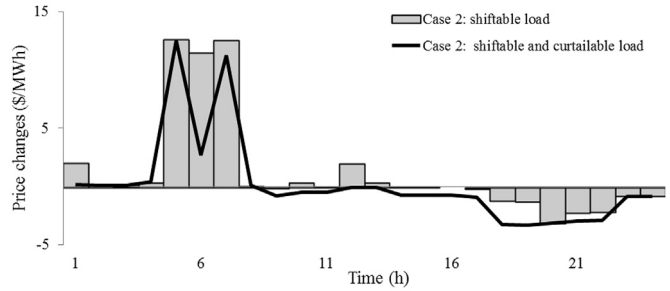

a) Stochastic wind power

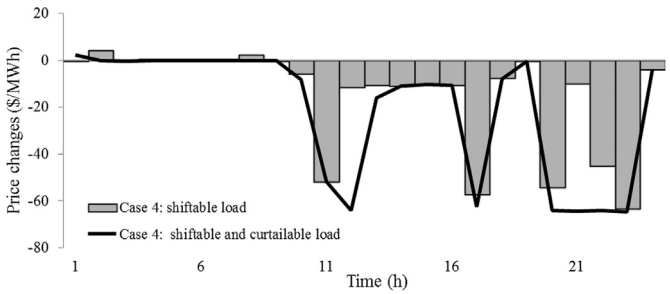

b) Stochastic wind power and N-1 contingencies

Fig. 7. Changes in market clearing price compared to base cases for the RTS-79.

Table 8
Optimal TOU rates ($/MWh) in case 2 for the RTS-96.

Bus no.	ρ_b^{LTP}	ρ_b^{OTP}	ρ_b^{PTP}
1-6, 8–10, 25–26, 28–29, 31–32, 49-58	19	21.7	21.7
13-16, 18–20, 27, 33, 37–40, 42–44, 61, 66, 68	16.4	16.4	19
7, 30, 34, 63–64, 67	19	19	19
62	19	19.8	20.5

Table 9
Optimal TOU rates ($/MWh) in case 4 for the RTS-96.

Bus no.	ρ_b^{LTP}	ρ_b^{OTP}	ρ_b^{PTP}
1–10, 13–14, 25–34, 37–38, 44	19	21.7	21.7
15–16, 18–20, 39–40, 42–43, 49–57, 61–64, 66–68	16.4	16.4	19
58	19	19	19

Table 10
Different terms of operation cost in case 3 and case 4 for the RTS-96.

Pricing scheme	Case 3: Flat rate	Case 4: Optimal TOU	
		Shiftable load	Shiftable and curtailable load
Startup cost ($)	41,309	42,630	41,183
Energy cost ($)	1,409,670	1,397,520	1,295,250
Capacity reserve cost ($)	36 931	41,086	40,237
Deployed reserve cost ($)	83,472	89,866	87,688
Emission cost ($)	1,003,990	968,140	908,560
FIT cost ($)	307,920	310,110	309,700
Load shedding cost ($)	647,700	328,750	168,480
Wind spillage cost ($)	11,397	7632	8344

other words, curtailabe load are an effective tool for managing the load and consequently price in peak period.

3.2. Modified IEEE RTS-96

The modified IEEE RTS-96 is a multi-area test system that is developed by linking various single RTS-79 areas. The modified IEEE RTS-96 has 78 thermal units, 120 branches, and 51 load buses with 8010 MW daily peak load. Moreover, five wind farms with a same capacity (600 MW) have been added to the system in order to evaluate the effectiveness of the proposed model in the face of wind power uncertainty. Therefore, the installed wind generation is 37.5% of the system peak load. Furthermore, five N-1 contingencies include the outages of generators at Buses 15, 25 and the outages of lines 14–16, 39–48, and 60–61. The generation unit's offers to provide the energy and up/down spinning reserve capacities are assumed similar to the IEEE RTS-79 system and all other required input parameters are considered the same as the previous assumptions. In this system, we use four scenarios to maintain the computational tractability of the proposed stochastic model. Tables 8 and 9 listed the obtaining optimal TOU tariffs for the modified IEEE RTS-96 system in case 2 and case 4, respectively.

The optimal TOU tariffs as a result of simultaneous scheduling of supply-side and demand-side resources to provide additional required flexibility in response to small fluctuations (i.e. wind power uncertainty) and large variations (i.e. network component contingencies) are illustrated in Tables 8 and 9. As it can be seen, the obtained tariffs for a number of buses are the same in different periods. This means that, DR implementation in such buses have low priority. Moreover, there are 6 buses with low priority for DR implementation in case 2 while there is just one bus with fixed tariffs in case 4. This is due to the fact that TSO must motivate the customers more and more in contingency events in comparison with wind power uncertainty. However, it should be noted that contingencies location and wind farms geographical position are the crucial factors in this matter.

In order to investigate the impacts of the proposed scheduling method on different terms of objective function, the simulation results in case 3 and case 4 for the IEEE RTS-96 are shown in Table 10.

As it can be observed, a day-ahead schedule with an operation cost of $ 3,542,390 is obtained in case 3 that refers to supply-side scheduling. Implementing an optimal TOU pricing scheme decreases the total operation cost to $ 3,185,734 using a typical load shift strategy. It is noteworthy that, if there is the possibility of just 5% load curtailment, the total operation cost is dropped by more than 10% equal to $ 2,859,442. The obtained results also revealed that enabling TOU pricing scheme can improve the system security and can facilitate the utilization of the available wind energy. By comparing case 3 with case 4, the load shedding cost is decreased by 49.24% and 73.98% because of the load shifting and load curtailment strategies, respectively. Moreover, the wind energy curtailment in case 4 is decreased by more than 33% while employing load shifting strategy, whereas the wind energy curtailment is diminished by 26.79% as a result of implementation of load curtailment strategy.

4. Conclusion

This paper proposed a flexible security-constrained scheduling framework to address simultaneous coordinated operation of supply-side and demand-side in the face of wind power uncertainty as well as network component contingencies. Here, demand-side was enabled using an optimal TOU pricing scheme and the model aims at minimizing the total operation costs considering pollutant emissions as well as security issues in electricity market environment. The obtained results revealed that as a result of coordinated scheduling of supply-side and demand-side, the total operation cost was decreased, the pollutant emission was reduced, and the system security was improved. It was also shown that the distribution of loads and geographical location of installed generation units over the power grid were two important factors in determination of optimal TOU tariffs. Moreover, simulation results evidenced that the load curtailment DR strategy was more effective in the case of contingency occurrences while the load shifting DR strategy was more useful for facilitating wind power integration. In addition, the results revealed that the proposed model affected the optimal scheduling of thermal units by forming a more flat net load profile. Such salient features made the proposed model an applicable tool for managing power system variations in response to wind power fluctuations as well as unexpected contingencies.

Nomenclature

Indices

b	Index of system buses
i	Index of generating unit
l	Index of transmission line
m	Segment index for linearized fuel cost
f	Index of wind farms
s	Index of scenarios
t, t'	Index of hours
NM	Number of segments for the piecewise linearized emission and fuel cost curves of units
NS	Number of wind power realization scenarios
NG	Number of generation units
NT	Number of hours under study
NB	Number of network buses
NWF	Number of wind farms

Parameters

$d_b^0(t)$	Initial electricity demand of bus b at hour t (MW)
$C_i^e(m)$	Slope of segment m in linearized fuel cost curve of unit i ($/MWh)

$\rho_b^0(t)$ Initial electricity price of bus b at hour t (\$/MWh)
C_{it}^U Offered capacity cost of up-spinning reserve provision of unit i in hour t (\$/MW)
C_{it}^D Offered capacity cost of down-spinning reserve provision of unit i in hour t (\$/MW)
C_{it}^{UE} Offered energy cost of up-spinning reserve provision of unit i in hour t (\$/MWh)
C_{it}^{DE} Offered energy cost of down-spinning reserve provision of unit i in hour t (\$/MWh)
$e_i^{SO_2}(m)/e_i^{NO_x}(m)$ Slope of segment m in linearized emission curve of unit i for SO_2 and NO_x pollutants (kg/MWh)
ECC^{SO_2}/ECC^{NOx} Environmental cost coefficient of SO_2 and NO_x pollutants (\$/kg)
$E(t,t')$ Elasticity of demand
$\underline{Em}_i$ Lower limit on the emission cost of unit i (\$/h)
$\underline{F}_i$ Lower limit on the fuel cost of unit i (\$/h)
$P_i^{\min}/P_i^{\max}$ Minimum/Maximum output limit (MW)
RU_i/RD_i Ramp up/down (MW/h)
C_i^{ST} Start-up cost of unit i (\$)
MUT_i/MDT_i Minimum up/down time (h)
$W_{fst}^{\max}$ Available wind power of wind farm f in hour t of scenario s (MWh)
$P_f^{install}$ Installed capacity of wind farm f (MW)
X_l Reactance of line l
$DR_b^{\max}$ Maximum response potential of bus b to TOU program
π_{FIT} FIT incentive value (\$/MWh)
π_{cur} Cost of wind power curtailment (\$/MWh)
ω_s Probability of wind power scenario s
$VOLL_{bt}$ Value of lost load at bus b in hour t (\$/MWh)

Variables

δ_{bts} Voltage angle at bus b in hour t of scenario s (rad)
F_{lts} Power flow through line l in hour t of scenario s (MW)
I_{it} Binary status indicator of generating unit i in hour t
LS_{bts} Involuntary load shedding in bus b at hour t of scenario s (MW)
$P_{it}^e(m)$ Generation of segment m in linearized fuel cost curve (MW)
$d_b(t)$ Modified demand of bus b in hour t after implementing TOU program (MW)
P_{it}^{tot} Total scheduled power of unit i in hour t (MW)
SR_{it}^U Scheduled up-spinning reserve of unit i in hour t (MW)
SR_{it}^D Scheduled down-spinning reserve of unit i in hour t (MW)
sr_{its}^U Deployed spinning reserve of unit i in hour t of scenario s (MW)
sr_{its}^D Deployed down-spinning reserve of unit i in hour t of scenario s (MW)
P_{ft}^{wind} Scheduled wind power of wind farm f in hour t (MW)
W_{fst}^{int} Integrated wind power of wind farm f in hour t of scenario s (MW)
W_{fst}^{curt} Curtailed wind power of wind farm f in hour t of scenario s (MW)
ρ_b^{OTP} Off-peak tariff rate of TOU program at bus b (\$/MWh)
ρ_b^{LTP} Low-load tariff rate of TOU program at bus b (\$/MWh)
ρ_b^{PTP} Peak tariff rate of TOU program at bus b (\$/MWh)

References

[1] Troy N, Denny E, O'Malley M. Base-load cycling on a system with significant wind penetration. IEEE Trans Power Syst 2010;25(2):1088–97.
[2] Holttinen H, Tuohy A, Milligan M, Lannoye E, Silva V, Muller S, et al. The flexibility workout: managing variable resources and assessing the need for power system modification. IEEE Power Energy Mag 2013;11(6):53–62.
[3] Papaefthymiou G, Grave K, Dragoon K. Flexibility options in electricity systems. 2014. Report. Available at: http://www.ecofys.com/en/publication/flexibility-options-in-electricity-systems/.
[4] National Renewable Energy Laboratory (NREL). Flexibility in 21st century power systems. 2014. Available at: www.nrel.gov/docs/.../61721.pdf.
[5] Nickell BM. Wind dispatchability and storage interconnected grid perspective, presentation for the U.S. department of energy wind and hydro power program. 2008. Available at: www.nationalwind.org/pdf/Nickellstoragestory-Public.pdf.
[6] Liu G, Tomsovic K. Quantifying spinning reserve in systems with significant wind power penetration. IEEE Trans Power Syst 2012;27:2385–93.
[7] Pozo D, Contreras J. A chance-constrained unit commitment with an n-k security criterion and significant wind generation. IEEE Trans Power Syst 2013;28(3):2842–51.
[8] Khodayar ME, Wu L, Shahidehpour M. Hourly coordination of electric vehicle operation and volatile wind power generation in SCUC. IEEE Trans Smart Grid 2012;3(3):1271–9.
[9] Daneshi H, Srivastava AK. Security-constrained unit commitment with wind generation and compressed air energy storage. IET Gener Transm Distrib 2012;6(2):167–75.
[10] Karami M, Shayanfar HA, Aghaei J, Ahmadi A. Scenario-based security-constrained hydrothermal coordination with volatile wind power generation. Renew Sustain Energy Rev 2013;28:726–37.
[11] Parvania M, Fotuhi-Firuzabad M. Demand response scheduling by stochastic SCUC. IEEE Trans Smart Grid 2010;1(1):89–98.
[12] Khodaei A, Shahidehpour M, Bahramirad S. SCUC with hourly demand response considering intertemporal load characteristics. IEEE Trans Smart Grid 2011;2(3):564–71.
[13] Nikzad M, Mozafari B, Bashirvand M, Solaymani S, Ranjbar AM. Designing time-of-use program based on stochastic security constrained unit commitment considering reliability index. Energy 2012;41(1):541–8.
[14] Sahin C, Shahidehpour M, Erkmen I. Allocation of hourly reserve versus demand response for security-constrained scheduling of stochastic wind energy. IEEE Trans Sustain Energy 2013;4(1):219–28.
[15] Morales JM, Conejo AJ, Perez-Ruiz J. Simulating the impact of wind production on locational marginal prices, power Systems. IEEE Trans Power Syst 2011;26(2):820–8.
[16] Aalami HA, Moghaddam MP, Yousefi GR. Demand response modeling considering interruptible/curtailable loads and capacity market programs. Appl Energy 2010;87:243–50.
[17] Schweppe FC, Caramanis MC, Tabors RD, Bohn RE. Spot pricing of electricity. Boston: MA: Kluwer; 1988.
[18] Bouffard F, Galiana FD. An electricity market with a probabilistic spinning reserve criterion. IEEE Trans Power Syst 2004;19(1):300–7.
[19] The IEEE reliability test system-1996. IEEE Trans Power Syst 1999;14:1010–20.
[20] Heydarian-Forushani E, Moghaddam MP, Sheikh-El-Eslami MK, Shafiekhah M, Catalão JPS. A stochastic framework for the grid integration of wind power using flexible load approach. Energy Convers Manag 2014;88:985–98.
[21] Behrangrad M, Sugihara H, Funaki T. Effect of optimal spinning reserve requirement on system pollution emission considering reserve supplying demand response in the electricity market. Appl Energy 2011;88:2548–58.
[22] Karki R, Hu P, Billinton R. A simplified wind power generation model for reliability evaluation. IEEE Trans Energy Convers 2006;21:533–40.
[23] Amjady N, Aghaei J, Shayanfar HA. Stochastic multi objective market clearing of joint energy and reserves auctions ensuring power system security. IEEE Trans Power Syst 2009;24:1841–54.
[24] Sutiene K, Makackas D, Pranevicius H. Multistage K-means clustering for scenario tree construction. Informatica 2010;21:123–38.